REACTIVE SINTERING OF $NbAl_3$

Paulo Iris Ferreira and Ricardo M. Leal Neto***

$NbAl_3$ based intermetallic alloys were obtained by reaction sintering of elemental powders. The influence of the powders particle size distribution, the compact composition and the reaction sintering thermal cycle on the sintered pellet porosity, microhardness and microstructure were investigated. Process conditions were carefully controlled for $NbAl_3$ compact composition, which resulted in 96% dense pellets. $NbAl_3$ was the major phase observed in these pellets and Nb_2Al was seldom encountered at triple grain boundaries. When the aluminum content was decreased from 75a/o to 42a/o two phases, $NbAl_3$ and Nb_2Al, were synthesized simultaneously. The amount of each phase, the porosity and the microhardness of the resulting pellets were dependent on the initial compact composition. An explanation for the reaction sintering process of these niobium aluminides is proposed.

INTRODUCTION

Ordered intermetallic aluminides are regarded as potential materials for structural applications at high temperature due to their excellent corrosion ;istance, relatively low density and high mechanical ength over a wide range of temperatures.[1,2] However, ; low ductility, the tendency to brittle fracture and the vironmental sensitivity of the mechanical strength, nerally observed in these alloys, have restricted their ictical use.[1,2,3,4]

Several investigations carried out in the last decade ve shown that many of these limitations could be enuated, or even eliminated, through macroalloying, croalloying processes, and thermal-mechanical treat- ınts.[1,2,5,6] These findings have renewed interest on the ysical metallurgy of these alloys and, as a conse- ence, extensive research work in this area is now ing done worldwide.

Various routes have been evaluated for the fabrication intermetallic alloys including conventional melt-cast- g-working,[7,8,9] rapid solidification[10,11,12] and powder metallurgy (P/M).[13,14,15] In this universe of processes, conventional P/M is an important approach for the attainment of high performance, complex geometry components. In general, rapidly solidified prealloyed intermetallic powders or ribbons are used as starting materials and consolidation is accomplished by hot extrusion or hot isostatic pressing. Although this approach is well established, it involves long process cycles and high sintering temperatures at considerably high cost.

An alternative powder processing technique known as reaction sintering, combustion synthesis or self-propagating high temperature synthesis is gaining increased attention.[16,17,18,19] An extensive review of this subject has been given by Munir and Anselmi - Tamburini.[20] By this method compounds with a sufficiently negative formation enthalpy can be synthesized through an exothermic reaction between elemental powders. Low processing temperatures, short processing times, relatively inexpensive equipment and flexibility in composition and microstructure control, make this alternative attractive. Recent investigations have demonstrated the success of reaction sintering for fabricating near full density nickel, iron and niobium aluminides.[21,22,23]

The Nb-Al phase diagram is characterized by the presence of three intermetallic phases Nb_3Al, Nb_2Al and $NbAl_3$. The $NbAl_3$ compound exhibits a low density ($4.54 g/cm^3$) and a high melting point (1680°C).[24,25]

*Director, Nuclear Material Directorate
**Research Engineer, Dept. of Materials Science and Engineering
IPEN-CNEN/SP, P.O. Box 11049 - Pinheiros (CEP 05422-970) Sao ulo, SP, Brazil

8-7463/93 0109-08 $00.75

Attention has been focused on $NbAl_3$ due mainly to its use as a protective coating for Nb and its alloys, since the brittleness, associated with its $D0_{22}$ structure has restricted its use in structural components. Recently, renewed attention has been directed towards niobium aluminides with emphasis on mechanical property improvement.

The objective of the present research was to investigate the use of exothermic reactions to fabricate niobium aluminides from elemental powders. Fine Nb and Al powders were used to promote compound formation. The effects of processing variables on the reaction sintering process were studied for the $NbAl_3$ composition. The influence of compact stoichiometry on the characteristics of reaction sintered pellets was investigated for aluminum content in the range 42a/o - 75a/o. Microstructural characterization and limited mechanical property measurements were carried out on reaction sintered pellets.

EXPERIMENTAL

Figure 1 gives a schematic representation of the procedure used in this work for the reaction sintering of niobium aluminides. Commercial gas atomized aluminum (ALCOA) and hydride-dehydride niobium (FTI-Lorena) powders were initially size classified by sieving and divided into fractions. The particle size distribution for each fraction selected was determined using a sedigraph and is shown in Figure 2. Scanning electron microscopy was utilized for the characterization of the powder morphology. Figure 3 shows electron micrographs illustrating the typical morphology of the niobium and aluminum powders. Aluminum particles are round or ligamental in shape with a number of small satellites on the surface. Niobium particles are angular in shape, characteristic of the hydride/dehydride process.

After classification and analysis, the powders were weighted in the desired proportion $m_{Al}/m_{Nb} = X$ (m_{Al} and m_{Nb} are the weights of aluminum and niobium, respectively) and mixed. The value of X was varied from 0.21 to 0.87, which corresponds to aluminide compositions ranging from 17.38w/o Al (42a/o Al) to 46.56w/o (75a/o Al), respectively.

The Al and Nb powder mixtures were homogenized individually in air using a Turbula operating at 35rpm

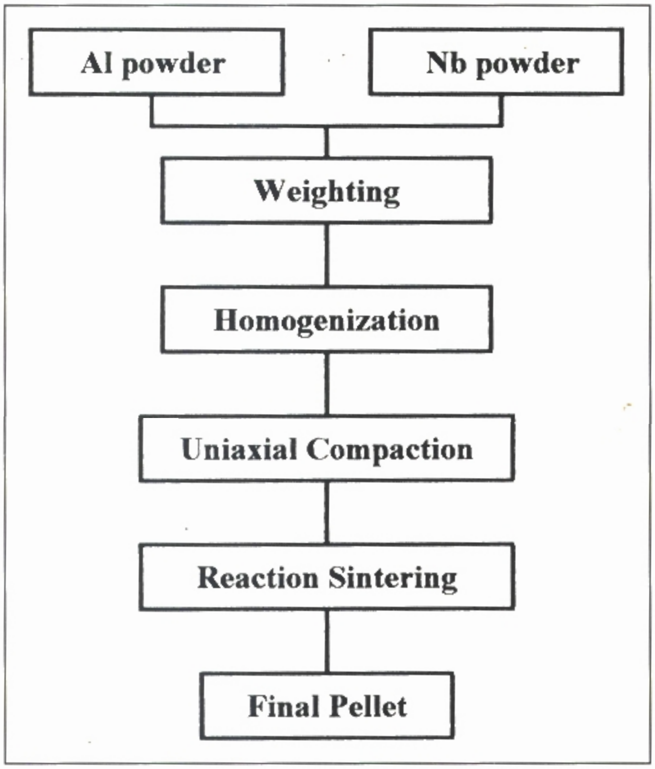

Figure 1. Schematic diagram illustranting the procedure used for reaction sintering.

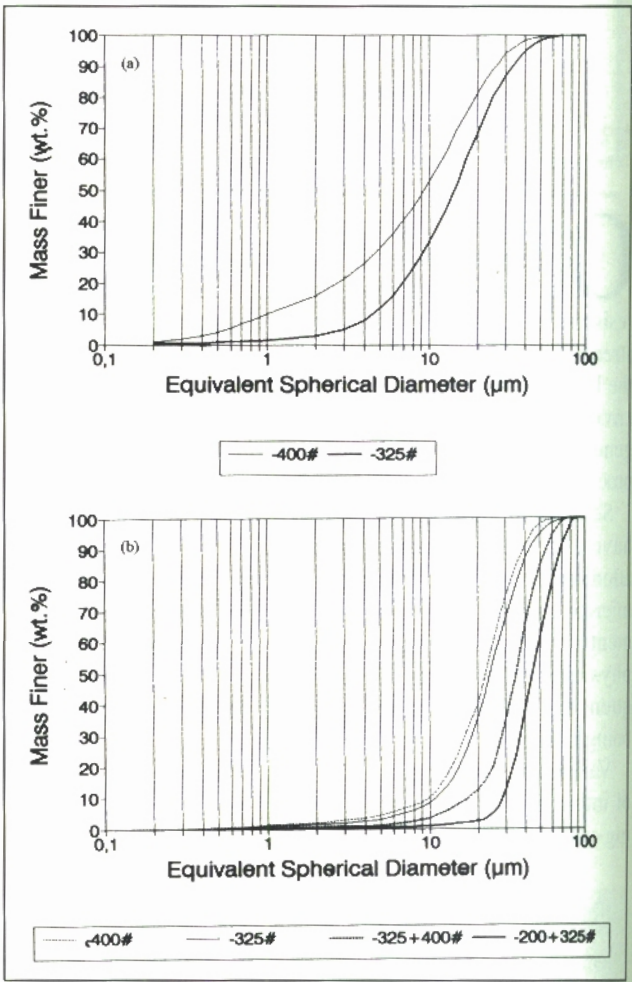

Figure 2. Particle size distributions: (a) niobium powder; and (b) aluminum powder.

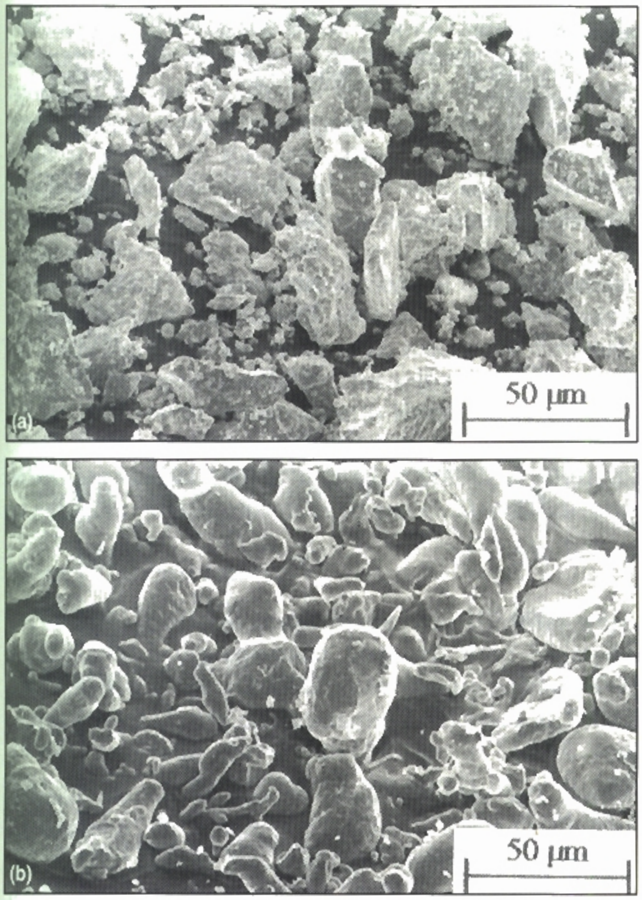

Figure 3. Micrographs of as received powder: (a) niobium; (b) aluminum; SEM.

for 10min. These conditions were appropriate for homogenization of the mixture of the various powder size distributions utilized. After this procedure, the powder mixtures were compacted at room temperature in an uniaxial press using a double acting die and applied pressures ranging from 200 to 400MPa. A solution containing stearic acid and acetone was used for die lubrication. Green compacts with 14mm external diameter and height about 6mm were obtained.

Reaction sintering of the compacts was conducted in a tubular furnace containing a moveable quartz chamber. The green compact was initially positioned in the interior of the chamber and the system evacuated until a pressure of 10^{-3}Pa was obtained. The chamber containing the compact was then introduced in the furnace before heating to the temperature T. Compact and furnace temperatures were monitored continuously and controlled with thermocouples. In all experiments a heating rate of 15°C/min was utilized. During the exothermic reaction, heat is liberated, leading to an increase in the compact temperature and a rapid transient in the vacuum level. The reacted compacts were kept in the furnace at the set temperature for 60min, and then cooled under vacuum by taking the quartz chamber off the furnace.

Longitudinal sections of the reaction sintered pellets were used for metallographic observations. The polished surfaces were analyzed using normal and polarized light techniques to reveal porous and grain structures, respectively.

SEM, X-ray diffraction and electron microprobe analysis were used for the characterization of the phases present in the sintered pellets as well as for their distribution. The bulk density of the pellets was determined by an immersion technique; total porosity could then be determined. Closed porosity was measured by means of a helium pycnometer.

EXPERIMENTAL RESULTS

Reaction Sintering of $NbAl_3$

The reaction sintering process was initially analyzed by differential thermal analysis (DTA). A $NbAl_3$ stoichiometric mixture of aluminum and niobium powder weighting 45.7mg was fed to the alumina crucible of the DTA equipment and tapped slightly. The experiment was run under argon atmosphere to minimize oxidation effects from 250°C to 1200°C at a heating rate of 15°C/min. A similar heating program was conducted with empty crucibles to establish a reference base.

The DTA curve obtained is presented in Figure 4. The first endothermic peak corresponds to melting of the aluminum. The exothermic reaction starts at approximately 900°C. Two peaks are clearly delineated: the first with a maximum around 950°C followed by the major peak around 1050°C. X-ray diffraction analysis confirmed $NbAl_3$ formation at the end of the exothermic reaction. This DTA curve was used as a reference for the planning of subsequent experiments.

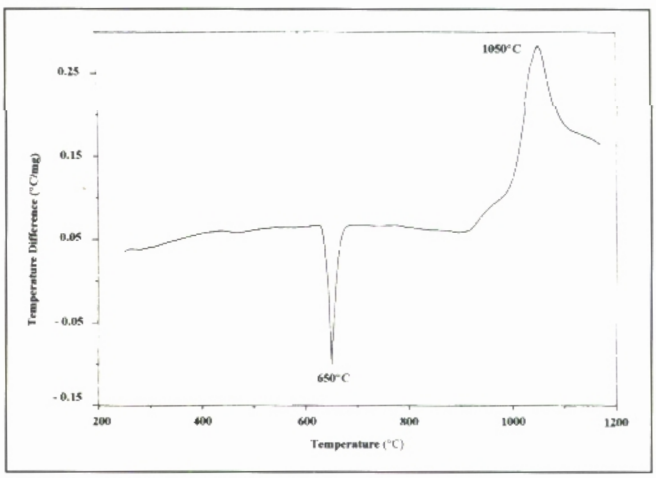

Figure 4. Differential thermal analysis (DTA) of Nb-Al mixture (75a/o Al).

TABLE I. Experimental Conditions Used in Reactive Sintering of $NbAl_3$.

Pellet Group	Powder Size Al	Powder Size Nb	Temperature and Time	Compacting Pressure (MPa)	Degassing (500°C/4h)	Relative Green Density
A	-325# (24μm)	-325# (15μm)	900°C/1h	200 300 400	No No No	85% 92% 94%
B	-325# (24μm)	-200+325# (55μm)	900°C/1h	200 300 400	No No No	88% 94% 96%
C	-325# (24μm)	-325# (15μm)	900°C/1h	300	Yes	92%
D	-400# (23μm)	-400# (9μm)	900°C/1h	300	Yes	92%
E	-200+325# (45μm)	- 400# (9μm)	1100°C/1h	300	Yes	92%
F	-325+400# (35μm)	-400# (9μm)	1100°C/1h	300	Yes	92%
G	-325# (24μm)	-325# (15μm)	1100°C/1h	300	Yes	92%
H	-400# (23μm)	-400# (9μm)	1100°C/1h	300	Yes	92%

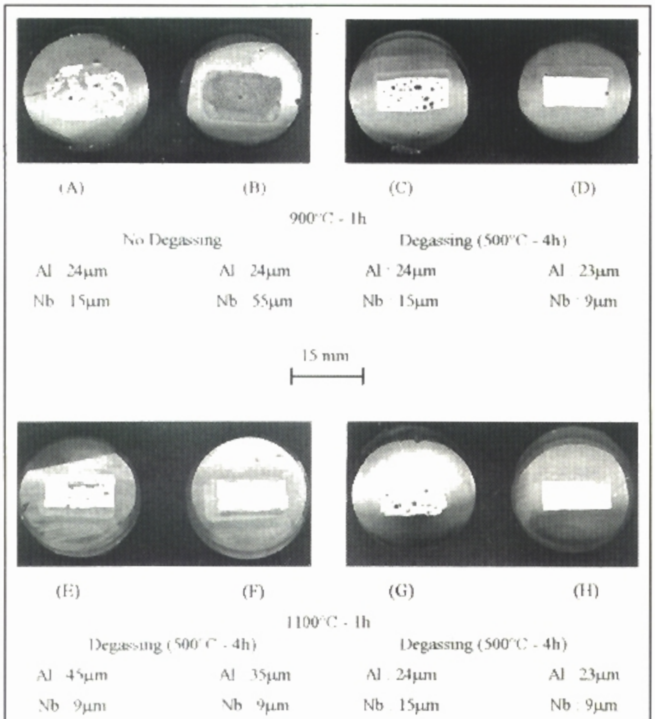

Figure 5. Optical macrographs of longitudinal sections of reaction sintered pellets processed for 1hr at 900°C (A to D) and 1100°C (E to H).

Table I summarizes the experimental conditions used for the initial investigation of the effects of the processing variables on the reaction sintering characteristics of $NbAl_3$. The variables were Al and Nb powder particle size distribution, furnace set temperature, compacting pressure and compact degassing.

Figure 5 shows typical macrographs of longitudinal sections of the reaction sintered pellets to illustrate the effect of processing variables on reaction sintering densification. In general, compaction pressure had no influence on the final pellet characteristics, at least in the range of pressures utilized in Table I.

The influence of degassing on densification can be seen via the observation of compacts fabricated under similar experimental conditions with average particle sizes of 24μm for Al, and 15μm for Nb, reaction sintered at 900°C. The macrographs (A and C) show clearly that without a degassing step, large voids are formed and general swelling of the reacted pellet takes place. Degassing leads to a considerable reduction in porosity, and only mild and uniform pellet swelling.

The influence of aluminum and niobium particle size on the reaction was investigated using compacts E to H. The green density was maintained at 92% theoretical. All compacts were degassed at 500°C/4hr and then heated to 1100°C under 10^{-3}Pa vacuum at a heating rate of 15°C/min. After the reaction transient, the pellets were kept at 1100°C for 1h and cooled to room temperature. Figure 5 illustrates the final porosity of those sintered pellets. Pellets E, F and H, for which the niobium particle size was kept constant (9μm) show that a large aluminum particle size resulted in the formation of large voids. Those large voids are also present if the niobium particle size is increased from 9µm to 15µm,. This can be seen from a comparison of the results obtained for compacts G and H. Similar behavior is observed for non-degassed compacts of groups A and B, reaction sintered at 900°C. In the particular case of pellet B the reaction was not completed and unreacted niobium remained, as confirmed by X-ray diffraction and microprobe analysis.

Above 900°C temperature, has only a small influence on densification, contrary to what is observed in classical sintering. Once the exothermic reaction is initiated, the heat generated is sufficient for self-propagation, and for the increase in temperature to levels where densification occurs. Increased densification is observed when pellets are held at 1100°C instead of 900°C, as illustrated in Figure 5 for compacts G, H and C, D, respectively.

Effect of Composition

The effects of stoichiometry on densification were investigated using compacts prepared from 23µm Al and 9µm Nb powder with a green density around 90% of theoretical. These compacts were degassed at 500°C for 4hr, heated in vacuum at 15K/min to 1100°C and held for 1hr. Figure 6 shows the levels of total and closed porosity after reaction, as a function of Al content. Total porosity decreases continually from around 30% to about 4% when the aluminum content is varied from 42a/o to the stoichiometric composition. Helium pycnometry data indicate that for compositions above the eutectic (54a/o Al), the majority of pores are closed, whereas at lower aluminum levels, interconnected porosity predominates.

Typical microstructures, observed under normal and polarized light conditions, for the pellets containing

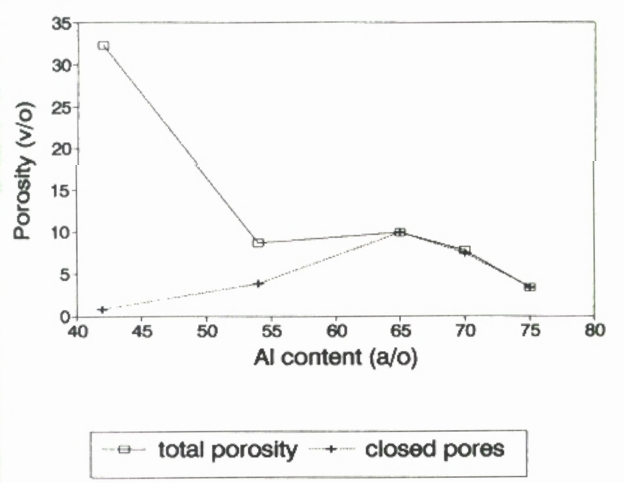

Figure 6. Total and closed porosity in reaction sintered pellets as a function of Al content.

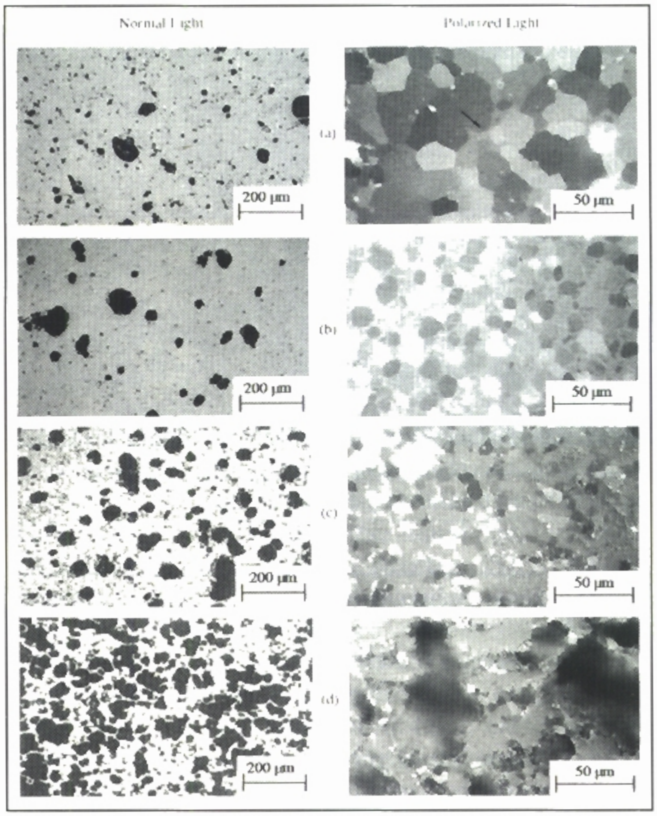

Figure 7. Optical micrographs taken under normal and polarized light, illustrating typical microstructures of sintered pellets with compositions: (a) 75 a/o Al; (b) 65 a/o Al; (c) 54 a/o Al; (d) 42 a/o Al.

42a/o, 54a/o, 65a/o and 75a/o Al, are presented in Figure 7. The pore structure occurring in the 75a/o. Al pellets is characterized by a bimodal distribution, Figure 7(a). Large pores with an average size ~ 50µm and very fine pores ~ 2µm in size are located preferentially at grain boundaries. When the aluminum content of the compact is decreased from 75a/o ($NbAl_3$) towards Nb_2Al, there is an increase in the amount and size of fine pores; thisresults in a sponge-like structure at 42a/o AC.

The major phase occurring at 75a/o Al is $NbAl_3$ as verified by X-ray diffraction and microprobe analysis. However, Nb_2Al phase is also observed in small areas, with a eutectic-like structure, located mainly at triple grain boundary joints, as indicated by the arrows in Figure 7(a) and Figure 8(a). Two phases, $NbAl_3$ and Nb_2Al, are always present in the pellets with a lower aluminum content.

Decreasing the amount of aluminum in the compact results in a reduction of $NbAl_3$ and an increase in Nb_2Al volume fractions. Volume fractions determined for each composition are consistent with values calculated from the equilibrium phase diagram. This can be visualized in Figure 7(a) to 7(d). The Nb_2Al phase is distributed in the

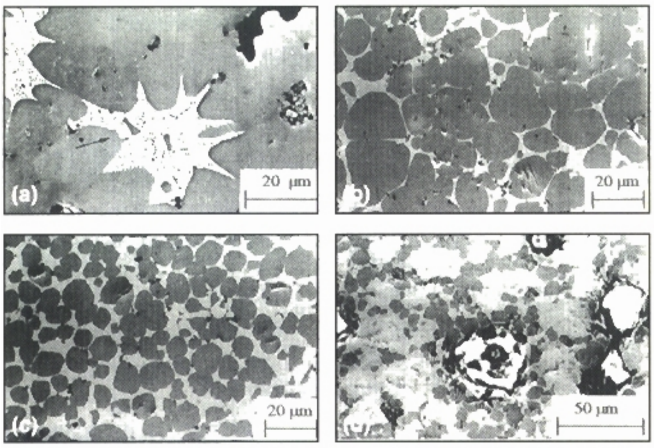

Figure 8. Micrographs of reaction sintered pellets: (a) 75 a/o Al; (b) 70 a/o Al; (c) 65 a/o Al; (d) 42 a/o Al, SEM.

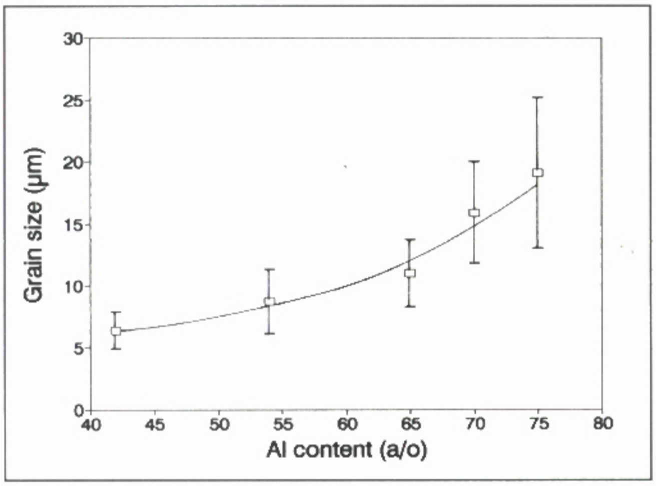

Figure 9. Average grain size of $NbAl_3$ in reaction sintered pellets as a function of Al content.

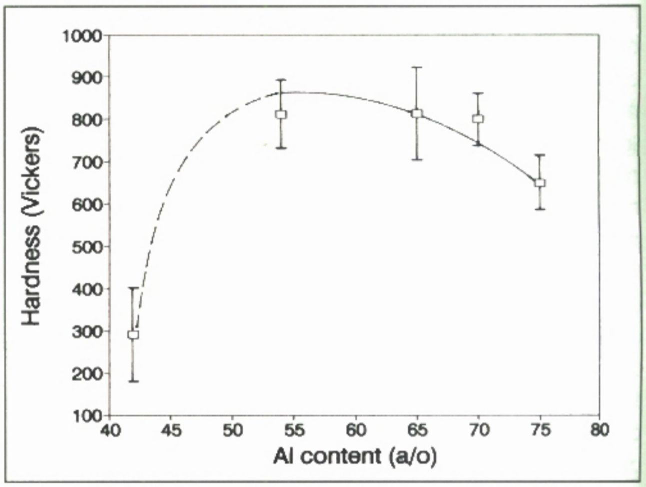

Figure 10. Vickers microhardness of reaction sintered pellets as a function of Al content.

microstructure in a thin slab along $NbAl_3$ grain boundaries at 70a/o Al, Figure 8(b). Furthermore, the $NbAl_3$ grains become increasingly spherical in shape. At 65a/o Al the microstructure consists of rounded $NbAl_3$ particles dispersed in a continuous Nb_2Al matrix, as illustrated in Figures 7(c) and 8(c). Compacts with a composition below the eutectic (54a/o Al) result in sintered pellets with a microstructure containing large continuous areas of Nb_2Al surrounded by $NbAl_3$ grains in a necklace morphology, as seen in Figures 7(d) and 8(d). There is a reduction in the $NbAl_3$ grain size in the sintered pellet when the amount of Al is decreased from 75a/o to 42a/o, as illustrated in Figure 9.

Microhardness

Microhardness measurements were made on reaction sintered pellets using a Vickers diamond pyramidal indentor with a 100g load. Higher loads were seen to induce cracks around the indentation and unacceptable scatter in the results. Hardness values were affected by pellet porosity. However, reliable data (taken in areas of visibly low porosity) were obtained for pellets reaction sintered at 1100°C. These values were (544±92)Hv, (593±65)Hv, and (650±64)Hv for $NbAl_3$ pellets in the conditions E,F and H, respectively. Although the data show some scatter, a perceptible decrease in hardness with increasing porosity exists. The value measured for the 96% dense pellet, H, exceeds the value 509Hv (measured with a 200g load) reported by Murray and German[23] for reactive hot isostatically pressed 98% dense $NbAl_3$ pellets. The reason for this discrepancy is not clear.

The variation of microhardness with aluminum content is shown in Figure 10. The low value at 42 a/o Al reflects the high porosity of the specimen, as shown in Figure 6. For the other points in Figure 10, porosity is relatively low and its effect on hardness can, in principle, be neglected. Therefore, when the aluminum content is decreased, the hardness increases towards values around 800Hv. This increase in hardness is associated with an increased volume fraction of Nb_2Al, and a reduction in $NbAl_3$ grain size, as can be seen from Figures 8 and 9.

DISCUSSION

Transient liquid phase sintering mechanisms can explain the reaction sintering process.[21,22,23] An important requirement for densification is the presence of a wetting liquid during the reaction. The amount, duration and distribution of the liquid phase at the reaction zone will determine the final sintered density. In reaction sintering the liquid phase has an extremely short existence, confined to the passage of the reaction front. The quantity of liquid available at the reaction zone depends essentially on compact composition. The distribution of the liquid phase in the microstructure is strongly dependent on the Nb:Al particle size ratio, since this ratio affects the interconnectivity of the niobium and aluminum phases. Interconnectivity of the two phases helps capillary action of the molten aluminum phase. It is believed that the capillary forces bond particles together at the initial stages of the reaction, resulting in higher final sintered density.

The results presented in Figure 5 were obtained using the following Nb:Al particle size ratios: 1:1.6 (compact A); 1:0.4 (compact B); 1:1.6 (compacts C and G); 1:2.6 (compacts D and H); 1:5 (compact E); and 1:3.9 (compact F). According to the model proposed by Kusy,[26] interconnectivity of the aluminum and niobium phases for $NbAl_3$ (73v/o Al in the compact) occurs when Nb:Al = 1:3. In this work, optimum densification took place when D and H values (for degassed compacts processed at 900°C and 1100°C), were Nb:Al = 1:2.6. Similar results were reported by Murray and German[23] for a Nb:Al ratio of approximately 1:3. These results indicate that the interconnectivity of phases plays an important role in the mechanism of reaction sintering densification. However, the absolute values of the particle size of each phase also affect densification, since diffusion times involved in the reaction may not be sufficient for complete reaction when large particles are used.

An attempt to explain the present observations on reaction sintering Nb-Al compacts can be advanced. During initial heating of the Nb-Al compact, aluminum-rich zones are preferentially formed in the Nb particles starting at the point of contact between Al and Nb particles. Low solid solubility of niobium in aluminum, as indicated by the equilibrium phase diagram,[25] as well as by the fact that the diffusion coefficient of aluminum in niobium and/or niobium compounds is greater than that of Nb in Al,[27] would justify this unbalanced atom flux. Solid state nucleation and growth of compounds can, therefore, occur at aluminum-niobium interparticle contacts during heating. Experiments performed by Slama and Vignes[27] showed that $NbAl_3$ is first nucleated at these contact points. These points will be favored sites for initial aluminum melting since localized additional heating occurs when a compound is being formed. Liquid aluminum pools formed at these sites are sucked rapidly to empty spaces nearby by capillary action. Liquid aluminum covers the available surface of the niobium particles. At this stage, $NbAl_3$ nuclei exist in the compact in equilibrium with local molten aluminum and unreacted solid aluminum and niobium.

When the temperature of the compact is increased, the solubility of niobium in liquid aluminum increases. Niobium dissolution in liquid aluminum occurs. Growth of $NbAl_3$ nuclei occurs either by consumption of the niobium enriched liquid, or by eventual aluminum diffusion to the Nb-$NbAl_3$ interface. The first exothermic peak observed in the DTA curve (Figure 4) at around 950°C could be associated with these events. Once a small quantity of Nb-enriched liquid is formed, a rapid increase in the reaction rate takes place. As the temperature of the compact is raised, more enriched liquid is formed with a supplementary increase in reaction rate, in such a way as to end in reaction self-propagation.

The high speed of the overall process suggests that the initial $NbAl_3$ nuclei existing at Nb-Al interparticle contacts, grow mainly by means of the niobium enriched-liquid, until all reagents are consumed. Occasionally, local unbalanced supersaturated niobium-enriched liquid can be trapped at interstices between impinging $NbAl_3$ particles. These liquid pools could be responsible for the eutectic-like structure (Nb_2Al-$NbAl_3$) observed at $NbAl_3$ triple grain boundary joints, Figure 8(a).

According to this model, outward currents of liquid aluminum would be flowing from the original aluminum particle sites. Also, a niobium-enriched aluminum current would be flowing in the opposite direction on the $NbAl_3$ particles surfaces. Neighboring $NbAl_3$ particles grow and contact. As a consequence, gross pores will be left at the original aluminum particle sites. Furthermore, fine porosity can occur at $NbAl_3$ grain boundaries due to the presence of entrapped liquid when $NbAl_3$ particles touch each other.

The present results are consistent with the proposed explanation. In fact, on increasing the aluminum particle size at a fixed niobium particle size (compacts H, F and E) the average size of the large pores observed in the microstructure also increases as expected. It is believed that the spherical voids observed in some areas of these reaction sintered pellets are the result of residual gas pressurization that occurs during the reaction, indicating that the degassing process is less efficient when large aluminum particle sizes are used. Another important point is that the fine porosity is almost exclusively located at $NbAl_3$ boundaries, Figures 7(a), 8(b), and 8(c). This reinforces the idea that $NbAl_3$ grains grow using the niobium-enriched liquid.

When the amount of niobium in the compact is increased, at least two things are expected. First, the niobium content of the liquid phase would increase to values required for Nb_2Al formation. Growth of this phase should occur intergranularly. In fact Nb_2Al occurs intergranularly as illustrated in Figure 8(b) and 8(c). Secondly, the number of Al-Nb interparticle contacts increases. Therefore, a larger number of $NbAl_3$ nuclei will be present in the compact during the initial stage of reaction sintering. These nuclei will be competing for aluminum in order to grow, resulting in a reduced final $NbAl_3$ grain size. This would explain the decrease in the final $NbAl_3$ grain size shown in Figure 9 when the amount of niobium in the compact is increased.

CONCLUSIONS

Reaction sintering was investigated as a pressureless process to synthesize high density niobium aluminides based upon the $NbAl_3$ stoichiometry. Compound synthesis occurs within seconds during rapid compact heating and is associated with the exothermic reaction. Best results were obtained with the following experimental conditions: a Nb:Al particle size ratio equal to 1:2.6; a heating rate of 15°C/min; a holding time at temperature of 1100°C/1 hour; a degassing step at 500°C/4h; and a vacuum level of 10^{-5} Torr. Microstructure of these 96% dense pellets is characterized by the presence of $NbAl_3$ grains; a very small quantity of Nb_2Al phase is also observed at triple grain boundaries. The effect of compact composition was investigated for aluminum contents varying from 42 a/o to 75 a/o. Two phases, $NbAl_3$ and Nb_2Al, are synthesized simultaneously when the niobium content of the compacts is increased towards the Nb_2Al stoichiometry. $NbAl_3$ nucleates first at niobium-aluminum interparticle contacts. The Nb_2Al phase occurs between the $NbAl_3$ grains when compact compositions are above the eutectic. Below the eutectic composition, $NbAl_3$ grains were seen to be pushed to Nb_2Al grain boundaries during solidification, forming a necklace distribution. Reaction processed pellets showed microhardness values significantly higher than in a previous study.

BIBLIOGRAPHY

1. *High Temperature Ordered Intermetallic Alloys*, Proc. Materials Research Society Symposium, Boston, Vol. 39, 1985, edited by C. C. Koch, C. T. Liu, and N. S. Stoloff, Materials Research Society, Pittsburgh, P. A.
2. *High Temperature Ordered Intermetallic Alloys II*, Proc. Materials Research Society Symposium, Boston, Vol. 81, 1987, edited by N. S. Stoloff, C. C. Koch, C. T. Liu and O. Izumi, Materials Research Society, Pittsburgh, P. A.
3. N. S. Stoloff and R. G. Davies, "The Mechanical Properties of Ordered Alloys", Prog. Mat. Sci., 1966, vol. 13, no. 1, p. 1.
4. M. J. Marcincowsky "The Relationship Between Atomic Order and the Mechanical Properties of Alloys", *Treatise on Materials Science and Technology, Vol. 5*, 1974, edited by H. Herman, Academic Press, New York, p. 181.
5. C. T. Liu, "Ordered Intermetallic Alloys - Brittle Fracture and Ductility Improvement", *Science of Advanced Materials*, 1990, edited by H. Weidershich and M. Meshii, ASM International Publication, USA, p. 423.
6. M. H. Yoo - "Deformation and Fracture of Ordered Intermetallic Compounds", ibid, p. 461.
7. C. T. Liu, C. L. White, "Dynamic Embritlement of Boron-Doped Ni_3Al Alloys at 600°C", Acta Metall., 1987, vol. 35, no. 3, p. 643.
8. T. Takasugi, O. Izumi, and N. Masahashi, "Electronic and Structural Studies of Grain Boundary Strength and Fracture in $L1_2$ Ordered Alloys - II. On the Effect of Third Elements in Ni_3Al Alloy", Acta Metall., 1985, vol. 23, no. 7, p. 1259.
9. G. Sauthoff, "Intermetallic Alloys - Overview on New Materials Developments for Structural Applications in West Germany", Zeitschrift für Metallkunde, 1990, vol. 81, no. 12, p. 855.
10. R. Ray and R. Ayer, "Microstructures and Mechanical Properties of Rapidly Solidified Niobium Aluminide ($NbAl_3$)", J. of Materials Science, 1992, vol. 27, p.1642.
11. S. Nourbakhsh and P. Chen, "Microstructure and Mechanical Properties of Rapidly Solidified and Annealed Ni-Al Intermetallic Alloys", Acta Metall., 1989, vol. 37, no. 6, p. 1373.
12. I. Baker, F. S. Ichishita, V. A. Surprerant and E. M. Schulson, "Rapidly Solidified and Annealed Powders of Ni_3Al", Metallography, 1984, vol. 17, no. 3, p. 299.
13. E.M. Schulson, "Structure, Properties and Potential Applications of Intermetallic Compounds Produced from Powders", Int. J. of Powder Metall., 1987, vol. 23, no. 1, p.25.
14. M. Nakamura and Y. Kaieda, "Microstructure and Mechanical Properties of Sintered TiAl", Powder Metallurgy, 1988, vol. 31, no. 3, p. 201.
15. P. I. Ferreira and G. M. Gonçalves, "Obtenção do Intermetálico Ni_3Al via Sinterização por Reação", *Proc. Annual Congress of the Brazilian Society for Metals (ABM), vol. 4*, 1990, Brazilian Society for Metals, São Paulo, Brazil, p. 469.
16. R. W. Rice, "Microstructural Aspects of Fabricating Bodies By Self- Propagating Synthesis", J. of Mateirials Science, 1991, vol. 26, p. 6533.
17. D. M. Bowden, P. J. Meschter, L. H. Yu, M. A. Meyers and N. M. Thadhani, "Synthesis of Novel Aluminide-Based Materials", J. of Metals, 1988, vol. 40, no. 9, p. 18.
18. R. M. Leal Neto and P. I. Ferreira, "Investigação Preliminar da Sinterização por Reação do Trialumineto de Nióbio, $NbAl_3$", *Proc. Powder Metallurgy Seminar*, 1991, Brazilian Society for

Metals (ABM), São Paulo, Brazil, p. 399.
19. Z. A. Munir, "Synthesis of High Temperature Materials by Self- Propagating Combustion Methods", Am. Ceram. Soc. Bull., 1988, vol. 67, no. 2, p. 342.
20. Z. A. Munir and V. Anselmi - Tamburini, "Self-Propagating Exothermic Reactions: The Synthesis of High-Temperature Materials by Combustion", Materials Science Reports, 1989, vol. 3, no. 7, p. 277.
21. A. Bose, B. W. Rabin and R. M. German, "Reactive Sintering Nickel Aluminide to Near Full Density", Powder Metall. Int., 1988, vol. 20, no. 3, p. 25.
22. B. H. Rabin and R. N. Wright, "Synthesis of Iron Aluminides from Elemental Powders: Reaction Mechanisms and Densification Behavior", Metall. Trans. A, 1991, vol. 22A, no. 2, p. 277.
23. J. C. Murray and R. M. German, "Reactive Sintering and Reactive Hot Isostatic Compaction of Niobium Aluminide $NbAl_3$", Metall. Trans. A, 1992, vol. 23A, no. 9, p.145.
24. C. E. Lundin, A. S. Yamamoto, "The Equilibrium Phase Diagram, Niobium (Columbium) - Aluminum", Trans. of the Metall. Soc. of AIME, 1966, vol. 236, no. 6, p. 863.
25. J. L. Jorda, R. Flukiger and J. Muller, "A New Metallurgical Investigation of the Niobium - Aluminum System", J. Less-Common Metals, 1980, vol. 75, p. 227.
26. R. P. Kusy, "Influence of Particle Size Ratio on The Continuity of Aggregates", J. of Appl. Phys., 1977, vol. 48, no. 12, p. 5301.
27. G. Slama and A. Vignes, "Difusion dans Les Aluminiures de Niobium", J. Less-Common Metals, 1972, vol. 29, p. 189.